



Sharif University of Technology

Scientia Iranica

Transactions B: Mechanical Engineering

<https://scientiairanica.sharif.edu>

Study of peristaltic transport of a dusty second-grade fluid in a curved configuration

H. Tariq^a, A.A. Khan^b, and S. Shah^{c,*}

a. Department of Mathematics, National University of Modern Languages, Islamabad, Pakistan.

b. Department of Mathematics and Statistics, International Islamic University, Islamabad, Pakistan.

c. Department of Mathematics, Government Degree College, Asghar Mall, Rawalpindi, Pakistan.

Received 10 September 2021; received in revised form 8 June 2022; accepted 9 May 2023

KEYWORDS

Curved channel;
Peristaltic flow;
Second-grade dusty
fluid.

Abstract. This study attempts to analyze the effect of diverse parameters of the peristaltic flow of second grade dusty fluid through a curved configuration. Stream function conversions are used to model the separate system of equations for the dust particles and fluid. The Perturbation technique is used to get the analytical solutions and the results are verified through graphs. It is noticeable that the trapped bolus, compresses both the dust particles and fluid with an increase in 'the second grade parameter'. Moreover, a surge in 'the Reynolds number' Re effects the bolus trapped in the lower portion of the channel for fluid. Decrement in the velocity is observed with a rise in 'the wave number' δ and 'the second grade parameter' α_1 .

© 2024 Sharif University of Technology. All rights reserved.

1. Introduction

Peristalsis is referred as the sinusoidal waves drifting along the tube walls, passages and channels. Many physiological systems naturally follow this mechanism. The fertile egg motion through the uterine tubes, ureters carrying urine, blood vessels are the few examples of peristaltic movement within a living being. This mechanism can be observed in many industrial situations as well. Peristaltic pumps are mounted in machines to transport fluids like slurry fluids, unpurified crude oil, chemicals etc. Blood movement activity in the heart-lung machine is also carried out by such pumps. Fluids around us are mostly non-Newtonian in nature. Due to the wide application of non-Newtonian

fluids and peristalsis, researchers gave much attention to study them extensively [1–15].

Over the past few years, fluid consisting of small dust granules have derived the attention of many researchers. Many paints available nowadays have powder, glitters and different materials suspended in them. Juices containing pulp, polluted water, infected urine, unpurified petroleum can be few examples of such fluids [16]. Crooke [17] investigated the dusty fluid model for various situations and by assuming diverse boundary conditions. Dusty fluid model was then studied by Charya [18]. Srinivasa Charya and Rudha Krishnama Charya [19] presented an article that investigated the dusty fluid under wall properties influence. They studied the flow rate and the trapping of the dusty fluid. Muthuraj et al. [20] studied the impressions of Magnetohydrodynamics (MHD) on the dusty fluid. They also investigated the chemical reaction influence on viscous fluid. Dusty fluid with viscoelastic properties was studied by Bhatti et al. [21].

* Corresponding author.

E-mail address: sajidshahmath313@gmail.com (S. Shah)

The surface of the passage in this study was considered to be porous. Few recent studies that deal with dusty fluids are [22–30].

In physiological systems, many glandular ducts, tubes are curved in nature. The investigators gave huge importance to the studies that involved curved passages and also exhibiting peristaltic motion. Ali et al. [31] investigated the peristaltic aspect of the fluid flowing past a curved passage. The wavelength was taken long to give an initial understanding of the problem. In a curved passage the MHD impact of the peristaltic fluid flow was examined by Hayat et al. [32]. Shehzad et al. [33] examined the effect of slip on the boundaries of the fluid flowing through a curved passage. The Sisko fluid with variable viscosity, in a curved configuration was studied by Bibi et al. [34]. Two phase movement of nanofluid was investigated by Nadeem and Shahzadi [35]. Recently, Riaz et al. [36] studied the fluid with nanoparticles suspended in it, flowing past a curved channel. The channel walls were considered to be porous and partial slip condition was imposed on the boundary. The flow of Williamson fluid flowing through a curved channel is examined by Rashid et al. [37].

Literature survey indicates that no effort has been made to study the effects of peristaltic second grade dusty fluid in a curved configuration. The present study intends to provide the missing links in this context. This study is an effort to investigate the behavior of dusty second-grade fluid in a curved passage. The initiative of this study is the hope that such a results may be applicable in many clinical applications.

2. Mathematical modeling

We have considered a 2D curved channel with thickness $2a$. Further, it is considered that the second grade fluid with dust grains embedded is flowing past with channel having (u, v) the radial (r) and axial (a) velocities of the fluid while (u_s, v_s) be the velocities of the dust grains (see Figure 1). The mathematical description of the upper and lower walls, provided by Ali et al. [31], of

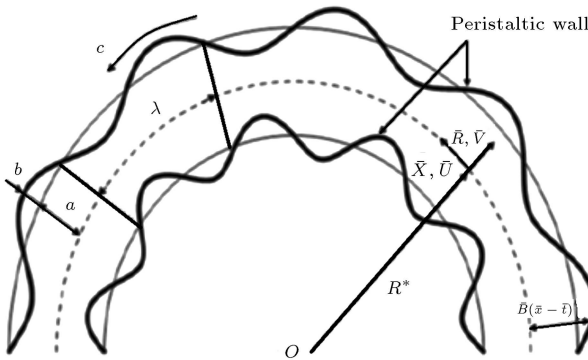


Figure 1. Curved configuration of the problem.

the channel is stated as:

$$\bar{H}(\bar{X}, t) = a + b \sin \frac{2\pi(\bar{X} - ct)}{\lambda}, \quad (1)$$

$$-\bar{H}(\bar{X}, t) = -a - b \sin \frac{2\pi(\bar{X} - ct)}{\lambda}. \quad (2)$$

The continuity equations are:

$$\left(R \frac{\partial}{\partial \bar{x}} + \frac{\partial}{\partial \bar{r}} (R + \bar{r}) \right) \bar{V} = 0, \quad (3)$$

$$\left(\frac{\partial}{\partial \bar{r}} (R + \bar{r}) + R \frac{\partial}{\partial \bar{x}} \right) \bar{V}_s = 0, \quad (4)$$

where the fluid's velocity is given by $\bar{V} = (\bar{u}, \bar{v})$ and the dust particle's velocity is $\bar{V}_s = (\bar{u}_s, \bar{v}_s)$. The constitutive momentum equations which governs the flow are given as:

$$\rho \left(\frac{\partial \bar{V}}{\partial t} + (\bar{V} \cdot \nabla) \bar{V} \right) = -\nabla \bar{P} + \nabla \bar{T} + lN(\bar{V}_s - \bar{V}), \quad (5)$$

$$\left(\frac{\partial \bar{V}_s}{\partial t} + (\bar{V}_s \cdot \nabla) \bar{V}_s \right) = \frac{l}{m} (\bar{V} - \bar{V}_s). \quad (6)$$

The number density of dust granules suspended in the fluid are considered to be constant. \bar{T} is the extra stress tensor of the second-grade fluid.

$$\bar{T} = \mu \bar{A}_1 + \bar{\alpha}_1 \bar{A}_2 + \bar{\alpha}_2 \bar{A}_1^2, \quad (7)$$

$$\bar{A}_1 = (\text{grad } \bar{V}) + (\text{grad } \bar{V})^t, \quad (8)$$

$$\bar{A}_2 = \frac{d\bar{A}_1}{dt} + \bar{A}_1 (\text{grad } \bar{V}) + (\text{grad } \bar{V})^t \bar{A}_1. \quad (9)$$

The reference frame (\bar{R}, \bar{X}) is converted into laboratory frame (\bar{r}, \bar{x}) by using the following conversions:

$$\begin{aligned} \bar{u}_s &= U_s - c, \quad \bar{v}_s = V_s, \quad \bar{x} = \bar{X} - ct, \\ \bar{r} &= \bar{R}, \quad \bar{u} = \bar{U} - c, \quad \bar{v} = \bar{V}. \end{aligned} \quad (10)$$

Below are the streamline functions and dimensionless quantities that have been used:

$$\begin{aligned} T &= \frac{a\bar{T}}{\mu c}, \quad u = \frac{\bar{u}}{c}, \quad A = \frac{lNa^2}{\mu}, \quad v_s = \frac{\bar{v}_s}{\delta c}, \\ \delta &= \frac{a}{\lambda}, \quad r = \frac{\bar{r}}{a}, \quad v = \frac{\bar{v}}{\delta c}, \quad u_s = \frac{\bar{u}_s}{c}, \\ Re &= \frac{\rho ca}{\mu}, \quad x = \frac{\bar{x}}{\lambda}, \quad \alpha_1 = \frac{c\alpha_1}{\mu a}, \quad P = \frac{a^2}{\lambda \mu c} \bar{P}, \\ v_s &= \frac{\Omega}{r + \Omega} \frac{\partial \phi}{\partial x}, \quad \Omega = \frac{R}{a}, \quad v = \frac{\Omega}{r + \Omega} \frac{\partial \psi}{\partial x}, \\ B &= \frac{la}{mc}, \quad u_s = -\frac{\partial \phi}{\partial r}, \quad u = -\frac{\partial \psi}{\partial r}. \end{aligned} \quad (11)$$

After removing the pressure terms, the compatibility

equations of the fluid and solid granules are as under:

$$\begin{aligned}
 & -\frac{\Omega}{r+\Omega} \frac{\partial^2 \psi}{\partial r^2} \frac{\partial \psi}{\partial x} + \frac{1}{(r+\Omega)^2} \frac{\partial \psi}{\partial x} \left(1 - \frac{\partial \psi}{\partial r}\right) \\
 & - \left(1 - \frac{\partial \psi}{\partial r}\right) \frac{1}{r+\Omega} \frac{\partial^2 \psi}{\partial x \partial r} \\
 & + \left(\frac{r}{\Omega} + 1\right) \frac{\partial^3 \psi}{\partial x \partial r^2} - \frac{\partial \psi}{\partial x} \frac{\partial^3 \psi}{\partial r^3} \\
 & - \left(\frac{r+\Omega}{\Omega}\right) \left(1 - \frac{\partial \psi}{\partial r}\right) \frac{\partial^2}{\partial r^2} \left(\frac{\partial \psi}{\partial x} \frac{\Omega}{\Omega+r}\right) \\
 & + \delta^2 \frac{\Omega}{\Omega+r} \frac{\partial^3 \psi}{\partial x^3} + \delta^2 \frac{2\Omega^2}{(\Omega+r)^3} \frac{\partial \psi}{\partial x} \frac{\partial^2 \psi}{\partial x^2} \\
 & - \delta^2 \frac{\Omega^2}{(\Omega+r)^2} \frac{\partial \psi}{\partial x} \frac{\partial^3 \psi}{\partial x^2 \partial r} + \frac{1}{\Omega} \frac{\partial^2 \psi}{\partial r \partial x} \\
 & - \delta^2 \frac{\partial^3 \psi}{\partial r^3} \frac{\Omega^2}{(\Omega+r)^2} \left(1 - \frac{\partial \psi}{\partial r}\right) \\
 & - \frac{\partial^2 \psi}{\partial r \partial x} \left(1 - \frac{\partial \psi}{\partial r}\right) \frac{2}{\Omega+r} \\
 & = \frac{1}{Re} \left(\frac{\partial^2}{\partial x \partial r} + \frac{\partial}{\partial x} \frac{1}{\Omega+r}\right) T_{xx} \\
 & + \frac{1}{\delta Re} \left[\frac{1}{\Omega} \frac{\partial}{\partial r} \left(\frac{1}{\Omega+r} \frac{\partial}{\partial r} (\Omega+r)^2\right) \right. \\
 & \left. - \delta^2 \frac{\Omega}{\Omega+r} \frac{\partial^2}{\partial x^2} \right] T_{rx} - \frac{1}{Re} \frac{1}{\Omega+r} \frac{\partial^2}{\partial r \partial x} [(r+\Omega) T_{rr}] \\
 & + \frac{1}{\delta Re} A \left[\left(\frac{1}{\Omega} \frac{\partial}{\partial r} + \frac{\Omega}{\Omega+r} \frac{\partial^2}{\partial r^2} + \delta^2 \frac{\partial^2}{\partial x^2} \right) (\psi - \phi) \right], \\
 & \frac{1}{\Omega} \frac{\partial^2 \phi}{\partial r \partial x} - \frac{1}{r+\Omega} \frac{\partial \phi}{\partial x} \frac{\partial^2 \phi}{\partial r^2} + \frac{1}{(\Omega+r)^2} \left(1 - \frac{\partial \phi}{\partial r}\right) \frac{\partial \phi}{\partial x} \\
 & - \frac{\partial \phi}{\partial x} \frac{\partial^3 \phi}{\partial r^3} - \left(1 - \frac{\partial \phi}{\partial r}\right) \frac{\partial^2 \phi}{\partial r \partial x} \frac{1}{\Omega+r} \\
 & + \left(\frac{r+\Omega}{\Omega}\right) \frac{\partial^3 \phi}{\partial x \partial r^2} - \frac{2}{\Omega} \frac{\partial^2 \phi}{\partial x \partial r} \left(1 - \frac{\partial \phi}{\partial r}\right) + \delta^2 \frac{\partial^3 \phi}{\partial x^3} \\
 & + \delta^2 \frac{\partial^2 \phi}{\partial x^2} - \delta^2 \frac{\partial^3 \phi}{\partial x^2 \partial r} - \delta^2 \frac{\partial^3 \phi}{\partial x^3} \left(1 - \frac{\partial \phi}{\partial r}\right) \\
 & \frac{\Omega}{\Omega+r} - \frac{\Omega}{\Omega+r} \left(1 - \frac{\partial \phi}{\partial r}\right) \frac{\partial}{\partial r} \left(-\frac{\Omega}{(\Omega+r)^2} \frac{\partial \phi}{\partial x} \right. \\
 & \left. + \frac{\partial^2 \phi}{\partial x \partial r} \frac{\Omega}{\Omega+r}\right)
 \end{aligned}$$

$$= \frac{1}{\delta} B \left[\frac{\Omega}{\Omega+r} \frac{\partial^2}{\partial r^2} + \frac{1}{\Omega} \frac{\partial}{\partial r} + \delta^2 \frac{\partial^2}{\partial x^2} \right] (\psi - \phi).$$

The elements of extra stress tensor are:

$$\begin{aligned}
 T_{rr} &= 2\delta \frac{\partial}{\partial r} \left(\frac{\Omega}{\Omega+r} \frac{\partial \psi}{\partial x} \right) \\
 &+ \alpha_1 \left[-2\Omega\delta^2 \frac{\partial^2}{\partial r \partial x} \left(\frac{1}{\Omega+r} \frac{\partial \psi}{\partial x} \right) \right. \\
 &+ \left(1 - \frac{\partial \psi}{\partial r}\right) \frac{2\delta^2 \Omega^2}{\Omega+r} \frac{\partial^2}{\partial x \partial r} \left(\frac{1}{\Omega+r} \frac{\partial \psi}{\partial x} \right) \\
 &+ \frac{2\Omega^4 \delta^4}{(\Omega+r)^4} \left(\frac{\partial^2 \psi}{\partial x^2} \right)^2 \\
 &+ 2\Omega\delta^2 \frac{\partial^2}{\partial r^2} \left(\frac{\Omega}{\Omega+r} \frac{\partial \psi}{\partial x} \right) \frac{\partial \psi}{\partial x} \frac{1}{\Omega+r} \\
 &+ 4\delta^2 \left(\frac{\partial}{\partial r} \left(\frac{\Omega}{\Omega+r} \frac{\partial \psi}{\partial x} \right) \right)^2 \\
 &- 2\delta^2 \frac{\Omega^2}{(\Omega+r)^2} \frac{\partial^2 \psi}{\partial r^2} \frac{\partial^2 \psi}{\partial x^2} \\
 &+ \left(1 - \frac{\partial \psi}{\partial r}\right) \frac{\partial^2 \psi}{\partial r^2} \frac{2}{\Omega+r} \\
 &- \frac{4\Omega^2 \delta^2}{(\Omega+r)^3} \frac{\partial}{\partial x} \frac{\partial \psi}{\partial x} \left(1 - \frac{\partial \psi}{\partial r}\right) \\
 &+ \frac{2}{(\Omega+r)^2} \left(1 - \frac{\partial \psi}{\partial r}\right)^2 \left. \right] \\
 &+ \alpha_2 \left[4\delta^2 \left(\frac{\partial}{\partial r} \left(\frac{\partial \psi}{\partial x} \frac{\Omega}{\Omega+r} \right) \right)^2 \right. \\
 &+ \left(\frac{\partial}{\partial r} \left(-\frac{\partial \psi}{\partial r} \right) + \delta^2 \frac{\partial^2 \psi}{\partial x^2} \frac{\Omega^2}{(\Omega+r)^2} \right. \\
 &\left. \left. - \left(1 - \frac{\partial \psi}{\partial r}\right) \frac{1}{\Omega+r} \right)^2 \right], \\
 T_{rx} &= -\frac{\partial^2 \psi}{\partial r^2} + \frac{\Omega^2 \delta^2}{(\Omega+r)^2} \frac{\partial^2 \psi}{\partial x^2} - \left(1 - \frac{\partial \psi}{\partial r}\right) \frac{1}{\Omega+r} \\
 &+ \alpha_1 \left[-\delta \frac{\partial^2 \psi}{\partial x \partial r} \frac{1}{\Omega+r} + \delta \frac{\partial^3 \psi}{\partial x \partial r^2} \right. \\
 &\left. - \delta^3 \frac{\partial^3 \psi}{\partial x^3} \frac{\Omega^2}{(\Omega+r)^2} - \delta \left(1 - \frac{\partial \psi}{\partial r}\right) \frac{\partial^3 \psi}{\partial x \partial r^2} \frac{\Omega}{\Omega+r} \right]
 \end{aligned}$$

$$\begin{aligned}
\psi &= -\frac{F}{2}, \quad \frac{\partial \psi}{\partial r} = -1, \quad \phi = -\frac{E}{2} \quad \text{at} \quad r = h = 1 + \Phi \sin(x) \\
\psi &= +\frac{F}{2}, \quad \frac{\partial \psi}{\partial r} = -1, \quad \phi = \frac{E}{2} \quad \text{at} \quad r = -h = -(1 + \Phi \sin(x))
\end{aligned} \tag{12}$$

Box I

$$\begin{aligned}
& + \delta^3 \left(1 - \frac{\partial \psi}{\partial r} \right) \frac{\partial^2}{\partial x^2} \left(\frac{\Omega}{\Omega + r} \frac{\partial \psi}{\partial x} \right) \frac{\Omega^2}{(\Omega + r)^2} \\
& + \delta \frac{\Omega}{(\Omega + r)^2} \left(1 - \frac{\partial \psi}{\partial r} \right) \frac{\partial^2 \psi}{\partial x \partial r} \\
& - \delta \frac{\partial \psi}{\partial x} \frac{\Omega}{\Omega + r} \frac{\partial^3 \psi}{\partial r^3} - \delta^3 \frac{\Omega^3}{(\Omega + r)^4} \frac{\partial \psi}{\partial x} \frac{\partial}{\partial x} \left(\frac{\partial \psi}{\partial x} \right) \\
& + \delta^3 \frac{\Omega^2}{(\Omega + r)^2} \frac{\partial \psi}{\partial x} \frac{\partial^2}{\partial r \partial x} \left(\frac{\partial \psi}{\partial x} \frac{\Omega}{\Omega + r} \right) \\
& + \delta \frac{\Omega}{(\Omega + r)^3} \frac{\partial \psi}{\partial x} \left(1 - \frac{\partial \psi}{\partial r} \right) + \delta \frac{\Omega}{(\Omega + r)^2} \frac{\partial \psi}{\partial x} \frac{\partial^2 \psi}{\partial r^2} \\
& + 2\delta \frac{\partial}{\partial r} \left(-\frac{\partial \psi}{\partial r} \right) \frac{\partial}{\partial r} \left(\frac{\Omega}{\Omega + r} \frac{\partial \psi}{\partial x} \right) \\
& - 2\delta^3 \frac{\Omega^2}{(\Omega + r)^2} \frac{\partial}{\partial r} \left(\frac{\Omega}{\Omega + r} \frac{\partial \psi}{\partial x} \right) \frac{\partial^2 \psi}{\partial x^2} \\
& + \frac{2\delta}{\Omega + r} \frac{\partial}{\partial r} \left(\frac{\Omega}{\Omega + r} \frac{\partial \psi}{\partial x} \right) \left(1 - \frac{\partial \psi}{\partial r} \right) \Bigg], \\
& + \alpha_2 \left[+ 4\delta^2 \left(\frac{\partial}{\partial r} \left(\frac{\partial \psi}{\partial x} \frac{\Omega}{\Omega + r} \right) \right)^2 \right. \\
& + \left(-\frac{\partial^2 \psi}{\partial r^2} - \left(1 - \frac{\partial \psi}{\partial r} \right) \frac{1}{\Omega + r} \right)^2 \\
& \left. + \delta^2 \frac{\partial^2 \psi}{\partial x^2} \frac{\Omega^2}{(\Omega + r)^2} \right],
\end{aligned}$$

and Eq. (12) obtained as shown in Box I.

Dimensionless E and F are time mean flow rate for dust granules and fluid and are given as below:

$$Q = F + 2, \tag{13}$$

$$F = - \int_{-h}^{+h} \frac{\partial \psi}{\partial r} dr, \tag{14}$$

$$Q_s = E + 2, \tag{15}$$

$$F_s = - \int_{-h}^{+h} \frac{\partial \phi}{\partial r} dr, \tag{16}$$

here Q and Q_s are dimensionless time mean flow.

3. Solution methodology

By considering the series solution for ϕ and ψ as:

$$\phi = \phi_0 + \delta \phi_1 + \mathcal{O}(\delta^2),$$

$$\psi = \psi_0 + \delta \psi_1 + \mathcal{O}(\delta^2),$$

$$F = F_0 + \delta F_1 + \mathcal{O}(\delta^2),$$

$$E = E_0 + \delta E_1 + \mathcal{O}(\delta^2). \tag{17}$$

3.1. Zeroth order system

The zeroth order system of equations are:

$$\begin{aligned}
& \frac{1}{\Omega} \frac{\partial}{\partial r} \left(\frac{1}{\Omega + r} \frac{\partial}{\partial r} (\Omega + r)^2 \right) T_{0rx} \\
& + A \left[\left(1 + \frac{r}{\Omega} \right) \frac{\partial^2}{\partial r^2} + \frac{1}{\Omega} \frac{\partial}{\partial r} \right] (\psi_0 - \phi_0) = 0, \tag{18}
\end{aligned}$$

$$B \left[\frac{1}{\Omega} \frac{\partial}{\partial r} + \left(1 + \frac{r}{\Omega} \right) \frac{\partial^2}{\partial r^2} \right] (\phi_0 - \psi_0) = 0, \tag{19}$$

$$\begin{aligned}
T_{xx} &= -2\delta \frac{\partial}{\partial r} \left(\frac{\Omega}{\Omega + r} \frac{\partial \psi}{\partial x} \right) \\
& + \alpha_1 \left[2\delta^2 \frac{\partial^2}{\partial r \partial x} \left(\frac{\Omega}{\Omega + r} \frac{\partial \psi}{\partial x} \right) - \delta^2 \frac{\partial^2}{\partial r \partial x} \right. \\
& \left(\frac{1}{\Omega + r} \frac{\partial \psi}{\partial x} \right) \frac{2\Omega}{\Omega + r} \left(1 - \frac{\partial \psi}{\partial r} \right) - 2 \left(-\frac{\partial^2 \psi}{\partial r^2} \right)^2 \\
& - 2\delta^2 \frac{\partial^2}{\partial r^2} \left(\frac{\Omega}{\Omega + r} \frac{\partial \psi}{\partial x} \right) \frac{\partial \psi}{\partial x} \frac{\Omega}{\Omega + r} \\
& - 2\delta^2 \frac{\Omega^2}{(\Omega + r)^2} \frac{\partial^2 \psi}{\partial r^2} \frac{\partial^2 \psi}{\partial x^2} \\
& + \frac{\partial^2 \psi}{\partial r^2} \left(1 - \frac{\partial \psi}{\partial r} \right) \frac{2}{\Omega + r} \\
& \left. + 4\delta^2 \left(\frac{\partial}{\partial r} \left(\frac{\partial \psi}{\partial x} \frac{\Omega}{\Omega + r} \right) \right)^2 \right]
\end{aligned}$$

where,

$$T_{0rx} = -\frac{\partial^2 \psi_0}{\partial r^2} + \frac{1}{\Omega + r} \left(\frac{\partial \psi_0}{\partial r} - 1 \right), \quad (20)$$

with

$$\psi_0 = -\frac{F_0}{2}, \quad \frac{\partial \psi_0}{\partial r} = -1, \quad \phi_0 = -\frac{E_0}{2},$$

$$\text{at } r = h = 1 + \Phi \sin(x),$$

$$\psi_0 = +\frac{F_0}{2}, \quad \frac{\partial \psi_0}{\partial r} = -1, \quad \phi_0 = +\frac{E_0}{2},$$

$$\text{at } r = -h = -(1 + \Phi \sin(x)). \quad (21)$$

3.2. First order system

The first order system of equations are as under:

$$\begin{aligned} & \frac{1}{\Omega} \frac{\partial^2 \psi_0}{\partial r \partial x} - \frac{\partial^2 \psi_0}{\partial r^2} \frac{1}{\Omega + r} \frac{\partial \psi_0}{\partial x} + \frac{\partial \psi_0}{\partial x} \frac{1}{(\Omega + r)^2} \\ & \left(1 - \frac{\partial \psi_0}{\partial r} \right) - \left(1 - \frac{\partial \psi_0}{\partial r} \right) \frac{1}{\Omega + r} \frac{\partial^2 \psi_0}{\partial r \partial x} \\ & + \frac{\partial^3 \psi_0}{\partial x \partial r^2} \left(1 + \frac{r}{\Omega} \right) - \frac{\partial^3 \psi_0}{\partial r^3} \frac{\partial \psi_0}{\partial x} \\ & - \left(1 + \frac{r}{\Omega} \right) \frac{\partial^2}{\partial r^2} \left(\frac{\Omega}{\Omega + r} \frac{\partial \psi_0}{\partial x} \right) \left(1 - \frac{\partial \psi_0}{\partial r} \right) \\ & - \frac{\partial^2 \psi_0}{\partial x \partial r} \frac{2}{\Omega + r} \left(1 - \frac{\partial \psi_0}{\partial r} \right) \\ & = \left(\frac{1}{\Omega + r} \frac{\partial}{\partial x} + \frac{\partial^2}{\partial r \partial x} \right) Re^{-1/2} T_{0xx} \\ & + \frac{1}{\Omega} \left[\frac{\partial}{\partial r} \left(\frac{1}{\Omega + r} \frac{\partial}{\partial r} (\Omega + r)^2 \right) \right] Re^{-1/2} T_{1rx} \\ & - \left[\frac{1}{\Omega + r} \frac{\partial^2}{\partial r \partial x} (\Omega + r) \right] Re^{-1/2} T_{0rr} \\ & + A Re^{-1/2} \left[\frac{r}{\Omega + r} \frac{\partial^2}{\partial r^2} + \frac{1}{\Omega} \frac{\partial}{\partial r} \right] (\psi_1 - \phi_1), \quad (22) \end{aligned}$$

$$\begin{aligned} & \frac{1}{\Omega} \frac{\partial^2 \phi_0}{\partial r \partial x} - \frac{\partial \phi_0}{\partial x} \frac{\partial^2 \phi_0}{\partial r^2} \frac{1}{\Omega + r} + \frac{1}{(\Omega + r)^2} \\ & \left(1 - \frac{\partial \phi_0}{\partial r} \right) \frac{\partial \phi_0}{\partial x} - \left(1 - \frac{\partial \phi_0}{\partial r} \right) \frac{1}{\Omega + r} \frac{\partial^2 \phi_0}{\partial x \partial r} \\ & + \frac{\partial^3 \phi_0}{\partial x \partial r^2} \left(1 + \frac{r}{\Omega} \right) - \left(1 + \frac{r}{\Omega} \right) \frac{\partial}{\partial r} \\ & \left(-\frac{\partial \phi_0}{\partial x} \frac{\Omega}{(\Omega + r)^2} + \frac{\Omega}{\Omega + r} \frac{\partial^2 \phi_0}{\partial r \partial x} \right) \left(1 - \frac{\partial \phi_0}{\partial r} \right) \end{aligned}$$

$$- \frac{2}{\Omega} \frac{\partial^2 \phi_0}{\partial r \partial x} \left(1 - \frac{\partial \phi_0}{\partial r} \right) - \frac{\partial \phi_0}{\partial x} \frac{\partial^3 \phi_0}{\partial r^3}$$

$$= B \left[\left(1 + \frac{r}{\Omega} \right) \frac{\partial^2}{\partial r^2} + \frac{1}{\Omega} \frac{\partial}{\partial r} \right] (\phi_1 - \psi_1), \quad (23)$$

where:

$$\begin{aligned} T_{0xx} = & \alpha_1 \left[2 \left(\frac{\partial^2 \psi_0}{\partial r^2} \right)^2 + \left(1 - \frac{\partial \psi_0}{\partial r} \right) \frac{\partial^2 \psi_0}{\partial r^2} \frac{2}{\Omega + r} \right] \\ & + \alpha_2 \left[\left(-\frac{\partial^2 \psi_0}{\partial r^2} - \left(1 - \frac{\partial \psi_0}{\partial r} \right) \frac{1}{\Omega + r} \right)^2 \right], \quad (24) \end{aligned}$$

$$\begin{aligned} T_{0rr} = & \alpha_1 \left[\frac{2}{\Omega + r} \left(1 - \frac{\partial \psi_0}{\partial r} \right) \right. \\ & \left. + \left(1 - \frac{\partial \psi_0}{\partial r} \right)^2 \frac{2}{(\Omega + r)^2} \right] + \alpha_2 \\ & \left[\left(-\frac{\partial^2 \psi_0}{\partial r^2} - \frac{1}{\Omega + r} \left(1 - \frac{\partial \psi_0}{\partial r} \right) \right)^2 \right], \quad (25) \end{aligned}$$

$$\begin{aligned} T_{1rx} = & -\frac{\partial^2 \psi_1}{\partial r^2} + \frac{1}{\Omega + r} \frac{\partial \psi_1}{\partial r} \\ & + \alpha_1 \left[\frac{\partial^3 \psi_0}{\partial x \partial r^2} - \frac{\Omega}{\Omega + r} \left(1 - \frac{\partial \psi_0}{\partial r} \right) \right. \\ & + \frac{\partial^2 \psi_0}{\partial r^2} \frac{\partial \psi_0}{\partial x} \frac{\Omega}{(\Omega + r)^2} + \frac{\partial^2 \psi_0}{\partial x \partial r} \left(1 - \frac{\partial \psi_0}{\partial r} \right) \\ & + \frac{\Omega}{(\Omega + r)^2} + \frac{\Omega}{(\Omega + r)^3} \frac{\partial \psi_0}{\partial x} \left(1 - \frac{\partial \psi_0}{\partial r} \right) \\ & - 2 \frac{\partial^2 \psi_0}{\partial r^2} \left(-\frac{\partial \psi_0}{\partial x} \frac{\Omega}{(\Omega + r)^2} + \frac{\Omega}{\Omega + r} \frac{\partial^2 \psi_0}{\partial x \partial r} \right) \\ & + \frac{2}{\Omega + r} \left(1 - \frac{\partial \psi_0}{\partial r} \right) \left(-\frac{\Omega}{\Omega + r} \frac{\partial \psi_0}{\partial x} \right. \\ & + \left. \frac{\partial^2 \psi_0}{\partial r \partial x} \frac{\Omega}{\Omega + r} \right) + \frac{\partial^2 \psi_0}{\partial x \partial r} \frac{1}{\Omega + r} - \frac{\Omega}{\Omega + r} \\ & \left. \frac{\partial^3 \psi_0}{\partial r^3} \frac{\partial \psi_0}{\partial x} \right], \quad (26) \end{aligned}$$

with:

$$\psi_1 = -\frac{F_1}{2}, \quad \frac{\partial \psi_1}{\partial r} = 0, \quad \phi_1 = -\frac{E_1}{2},$$

$$\text{at } r = h = 1 + \Phi \sin(x),$$

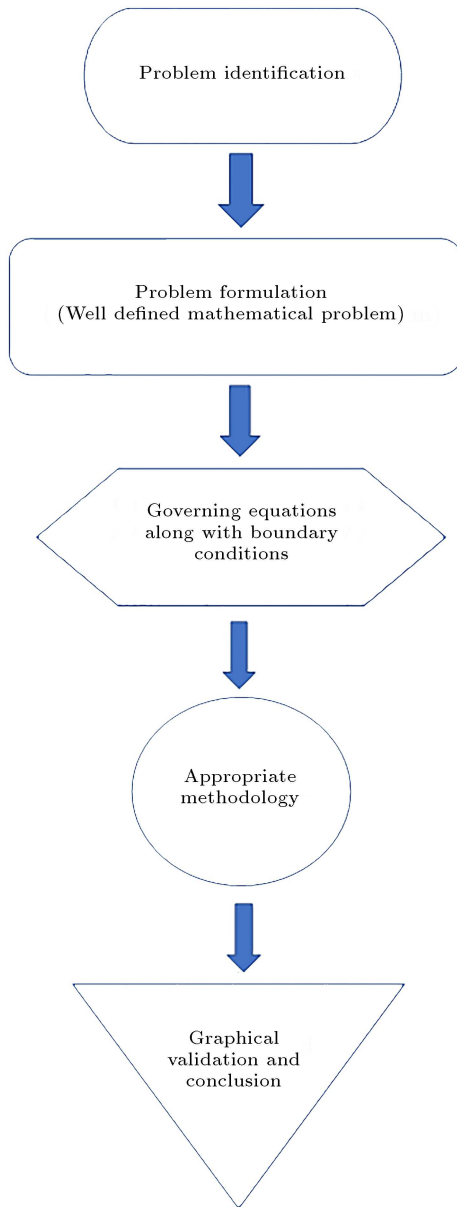


Figure 2. Flow chart of the problem

$$\psi_1 = +\frac{F_1}{2}, \quad \frac{\partial \psi_1}{\partial r} = 0, \quad \phi_1 = +\frac{E_1}{2},$$

at $r = -h = -(1 + \Phi \sin(x))$. (27)

DSolver command in Mathematica software have been utilized to get the solutions and graphs of the above mentioned system of equations.

Figure 2 display the flow chart that describes the pattern of complete manuscript.

4. Results interpretation

The results obtained analytically are plotted to check the validity and effects of physical parameters on the velocity and streamlines of the dusty second grade

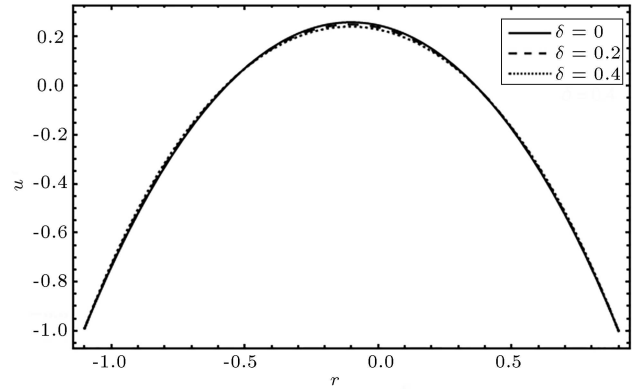


Figure 3. Fluid velocity for the parameter δ with $B = 0.7$, $\phi = 0.4$, $Q = 1.5$, $Re = 5$, $A = 0.8$, $\Omega = 3.5$, $Q_s = 1.8$, $\alpha_1 = 1$.

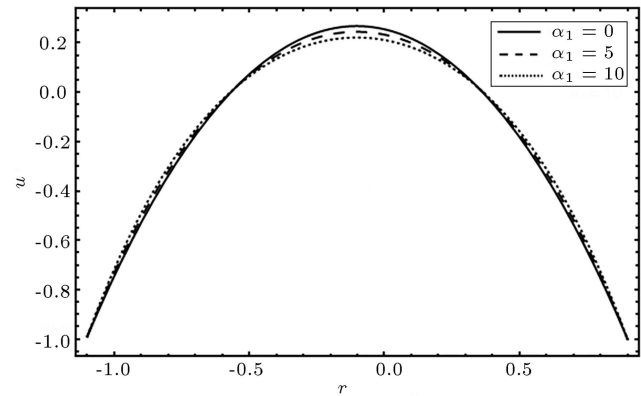


Figure 4. Fluid velocity for the parameter α_1 with $B = 0.7$, $\phi = 0.4$, $Q = 1.5$, $Re = 5$, $A = 0.8$, $\Omega = 3.5$, $Q_s = 1.8$, $\delta = 1$.

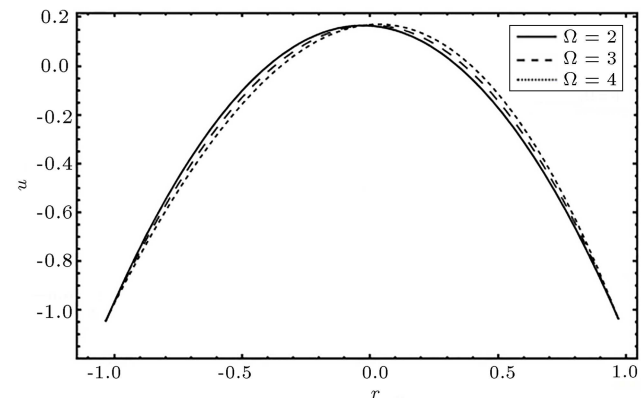


Figure 5. Fluid velocity for the parameter Ω with $B = 0.8$, $\phi = 0.45$, $Q = 1.5$, $Re = 8$, $A = 0.8$, $\delta = 1$, $Q_s = 1.8$, $\alpha_1 = 0.8$.

fluid. Figures 3–7 show the impact of wave number δ , curvature parameter Ω and the second-grade parameter α_1 on the fluid and dust grains velocity.

4.1. Velocity

In Figure 3, the effect of wave number can be observed. At the center of the passage, fluid's velocity decreases

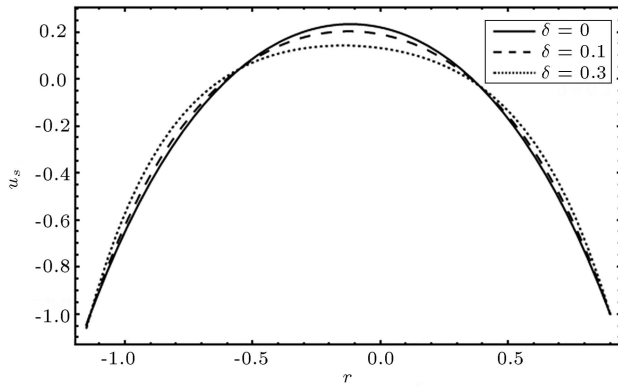


Figure 6. Dust granules velocity for the parameter δ with $B = 0.7$, $\phi = 0.4$, $Q = 1.5$, $Re = 5$, $A = 0.8$, $\Omega = 3.5$, $Q_s = 1.8$, $\alpha_1 = 1$.

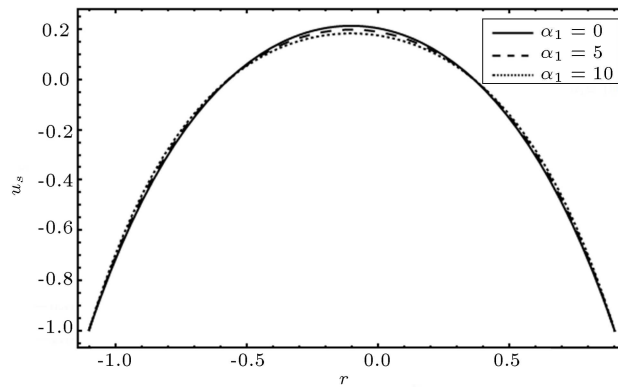


Figure 7. Dust granules velocity for the parameter α_1 with $B = 0.7$, $\phi = 0.4$, $Q = 1.5$, $Re = 5$, $A = 0.8$, $\Omega = 3.5$, $Q_s = 1.8$, $\delta = 0.01$.

as wave number has an inverse relation to wavelength thus with the increase in wave number, decrease in wavelength happens thus causing lesser turbulence and resulting reduction in fluid velocity. For the higher value of second-grade parameter, the fluid velocity drops as shown in Figure 4. Decline in the center of

the passage is spotted with the increase in second-grade parameter, this may be because second grade parameter affects the viscous nature of the fluid thus causing difficulties for it to flow. Figure 5 shows the impact of the curvature parameter on the velocity profile. A decline in the velocity is observed along the lower portion of the channel as the values of the curvature are increased. An opposite behavior emerges near the centerline of the channel that is the velocity inclines along the upper portion of the channel. Figure 6 demonstrates the impression of the velocity of solid dust particles under the effect of the wave number. The velocity at the boundaries remains unchanged while at the center of the channel, velocity declines with an enhance in the wave number. Surge in the second-grade parameter lowers down dust granules velocity as given in Figure 7.

4.2. Streamline patterns

4.2.1. For fluid

Streamline patterns are a useful tool to understand the flow of the fluid. Figure 8 portrays to see the effect of ‘the Reynolds number’, ‘ Re ’ on the trapped bolus of the fluid. The bolus trapped shrinks with the higher parametric values of Re in upper part of the channel while in the lower part it contracts and gradually vanishes. With the increase in Reynolds number, the effect of viscosity declines thus the trapped bolus flows past the curved configuration more steadily. In Figure 9 the impact of ‘the curvature parameter’ ‘ Ω ’ on streamlines can be observed. In upper part of the channel, the bolus compresses while formation of bolus can be seen in the bottom of the channel. One can deduce that rise in the curvature parameter may cause unsteadiness in the fluid flow. Figure 10 is disclosed to observe the impact of ‘the second-grade parameter’ ‘ α_1 ’ on the fluid’s trapped bolus. From Figure 10, it is witnessed that the viscous nature of fluid is enhanced

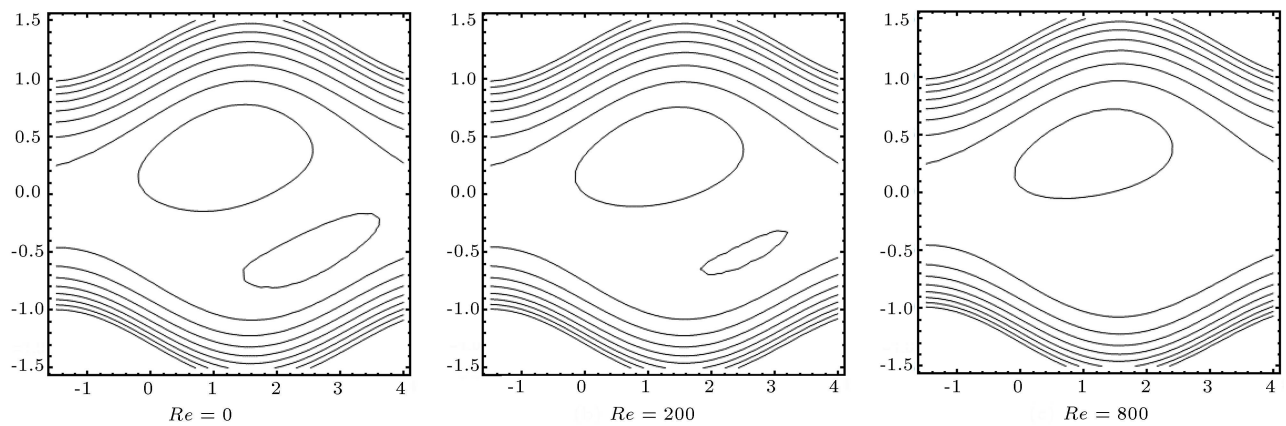


Figure 8. Fluid streamlines for the parameter Re with $B = 0.7$, $\phi = 0.15$, $Q = 5$, $A = 0.8$, $\Omega = 7$, $Q_s = 1.8$, $\delta = 0.01$, $\alpha_1 = 0.5$.

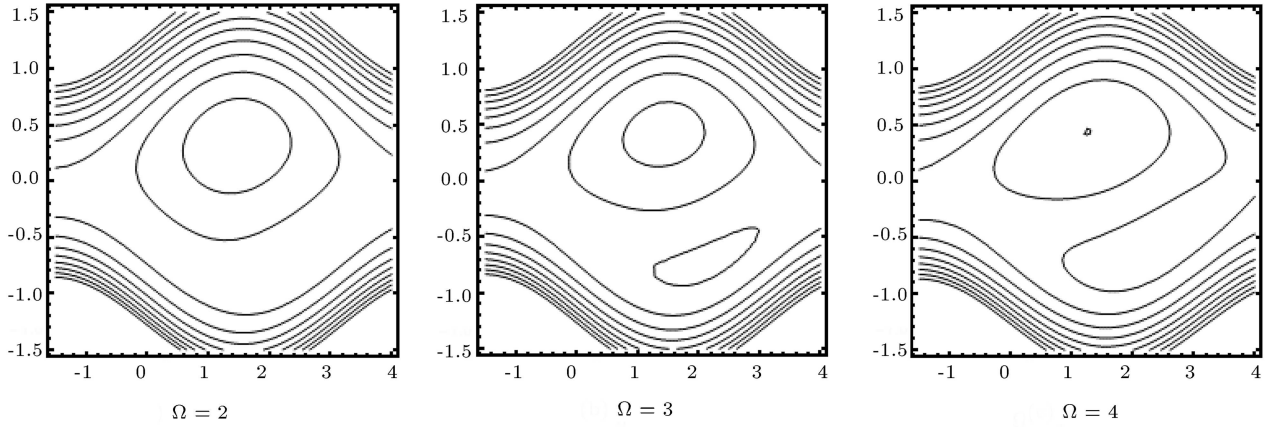


Figure 9. Fluid streamlines for the parameter Ω with $B = 0.7$, $\phi = 0.4$, $Q = 1.5$, $A = 0.8$, $Re = 5$, $Q_s = 1.8$, $\delta = 0.01$, $\alpha_1 = 2$.

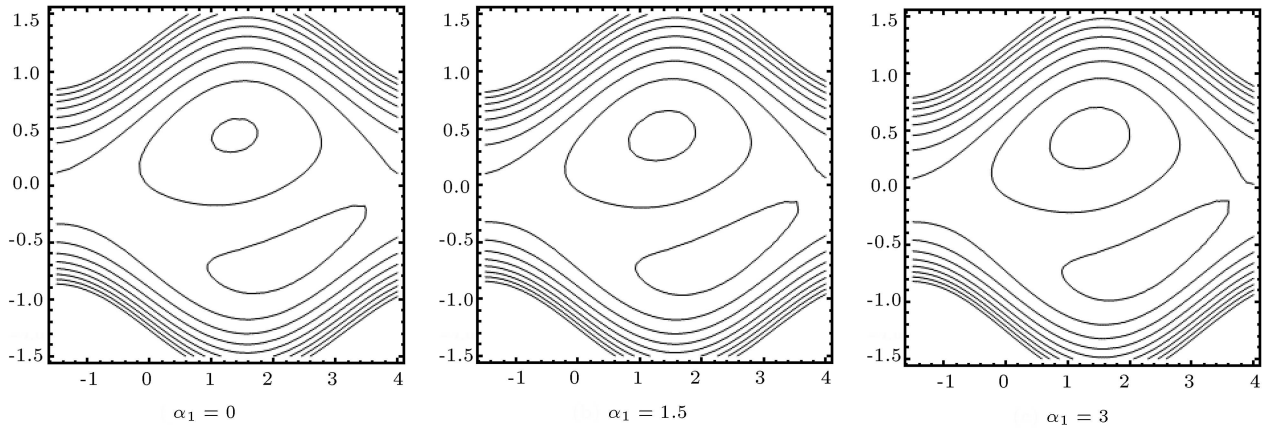


Figure 10. Fluid streamlines for the parameter α_1 with $B = 0.7$, $\phi = 0.4$, $Q = 1.5$, $A = 0.8$, $Re = 5$, $Q_s = 1.8$, $\delta = 0.01$, $\Omega = 3.5$.

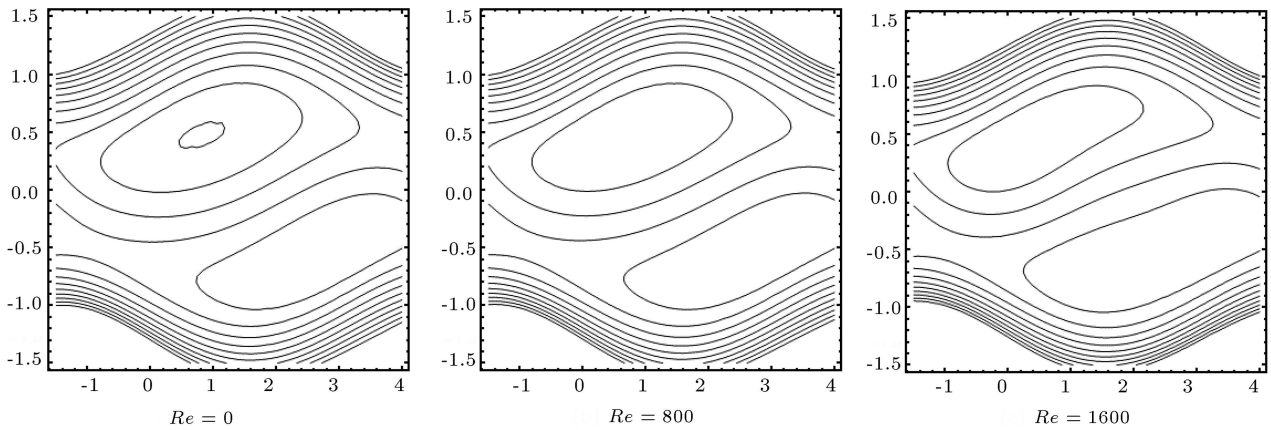


Figure 11. Dust granules streamlines for the parameter Re with $B = 0.7$, $\phi = 0.3$, $Q = 1.5$, $A = 0.8$, $\alpha_1 = 3$, $Q_s = 1.8$, $\delta = 0.02$, $\Omega = 4$.

for an increase in α_1 and hence the trapped bolus in the upward part of the channel grows in its size.

4.2.2. For solid particles

The bolus in the bottom part of the channel gets bigger with higher values of ‘the Reynolds number’ ‘ Re ’ as

depicted in Figures 11 and 12 is displaying the impact of ‘the curvature parameter’ ‘ Ω ’ on the streamlines of the dust particles. It is observed that in the lower section of the passage, a bolus forms with an upturn in Ω which continues to be growing with the rise in Ω . Due the increase in curvature parameter, the trapped

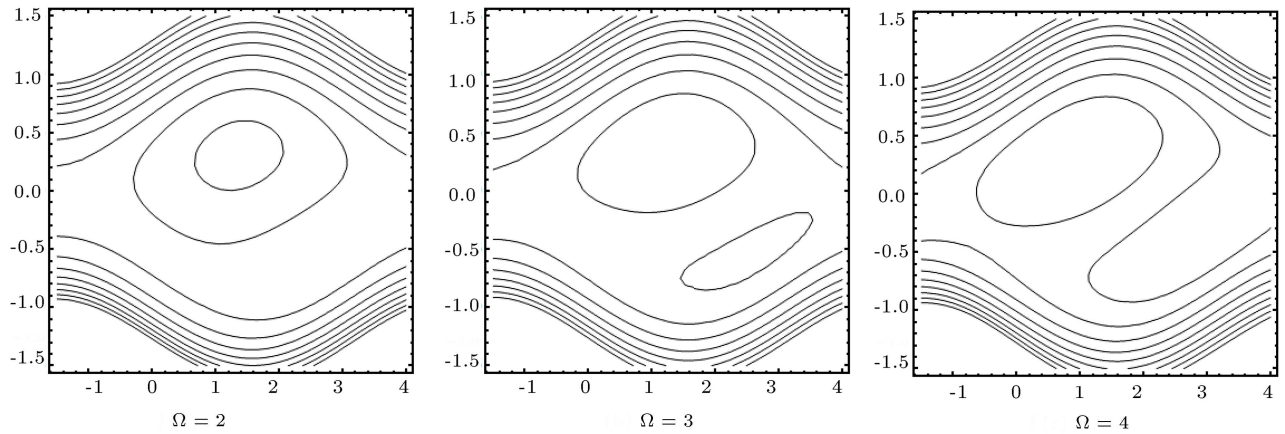


Figure 12. Dust granules streamlines for the parameter Ω with $B = 0.7$, $\phi = 0.3$, $Q = 1.5$, $A = 0.8$, $\alpha_1 = 2$, $Q_s = 1.8$, $\delta = 0.01$, $Re = 5$.

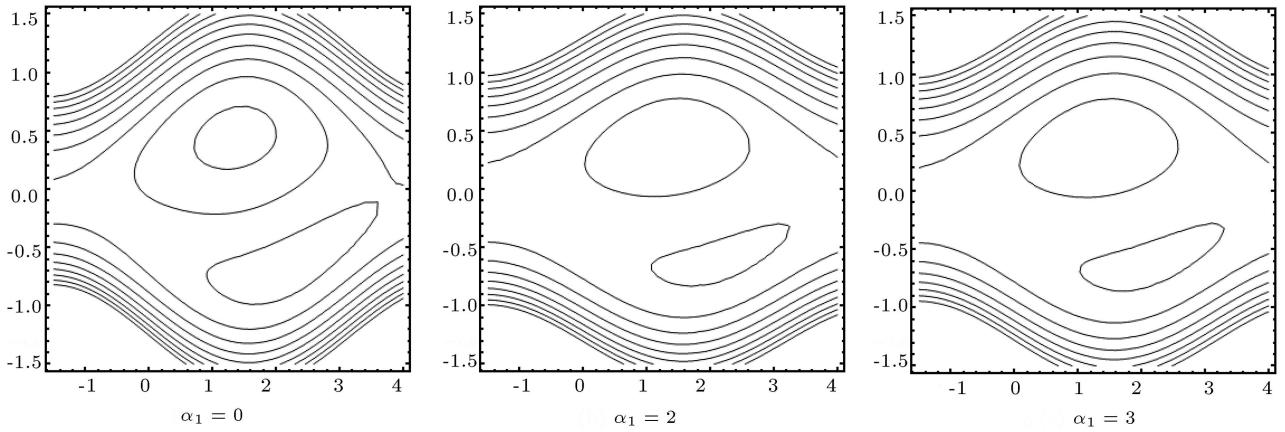


Figure 13. Dust granules streamlines for the parameter α_1 with $B = 0.7$, $\phi = 0.3$, $Q = 1.5$, $A = 0.8$, $\Omega = 4$, $Q_s = 1.8$, $\delta = 0.01$, $Re = 5$.

bolus is not symmetrical in upper and lower part of channel. A rise in ‘the second-grade parameter’ ‘ α_1 ’ causes contraction in the volume of the trapped bolus as demonstrated in Figure 13.

5. Concluding remarks

In a curved configuration, the peristaltic activity of second-grade dusty fluid is discussed. The results are obtained by using perturbation technique. Few notable points are given below:

- For fluid and dust particles formation of bolus can be spotted in the bottom part of the channel with increase in Ω ;
- The curvature parameter Ω enhances the velocity of the fluid in the right side of the channel;
- The trapped bolus contracts with the surge in the second-grade parameter α_1 for both solid and fluid particles;

- The trapped bolus in the lower portion of channel eventually vanishes with an increase in Re for fluid;
- A decay in the velocity of the dust grains and fluid is witnessed for an augmentation in the wave number δ and second-grade parameter α_1 .

This work can be extended by adding various body forces to this model.

Nomenclature

A, B	Non-dimensional parameters $A = \frac{lNa^2}{\nu}$, $B = \frac{la}{mc}$
a	Channel thickness
b	Wave amplitude
c	Wave speed
l	Stokes’s co-efficient of resistance
m	Mass of the solid particles
N	Number density of solid particles

Re	Reynolds number
\bar{T}	Extra stress tensor in reference frame
T	Extra stress tensor in laboratory frame
\bar{t}	Time in reference frame
(\bar{U}, \bar{V})	Fluid velocities in reference frame
(\bar{U}_s, \bar{V}_s)	Dust particles velocities in reference frame
(U, V)	Fluid velocities in laboratory frame
(U_s, V_s)	Dust particles velocities in laboratory frame
(u, v)	Non-dimensional velocities of fluid
(u_s, v_s)	Non-dimensional velocities of dust particles
α_1	Second-grade parameter in dimensionless form
Ω	Curvature of the channel
δ	Wave number
λ	Wavelength
ρ	Fluid density

References

- Shapiro, A.H., Jaffrin, M.Y., and Weinberg, S.L. "Peristaltic pumping with long wavelengths at low Reynolds number", *Journal of Fluid Mechanics*, **34**(4), pp. 799–825 (1969).
- Bhatti, M.M. and Abdelsalam, S.I. "Bio-inspired peristaltic propulsion of hybrid nanofluid flow with Tantalum (Ta) and Gold (Au) nanoparticles under magnetic effects", *Waves in Random and Complex Media*, pp. 1–26 (2021).
- Bhatti, M.M., Zeeshan, A., Bashir, F., et al. "Sinusoidal motion of small particles through a Darcy-Brinkman-Forchheimer microchannel filled with non-Newtonian fluid under electro-osmotic forces", *Journal of Taibah University for Science*, **15**(1), pp. 514–529 (2021).
- Ramadan, S.F., Mekheimer, K.S., Bhatti, M.M., et al. "Phan-Thien-Tanner nanofluid flow with gold nanoparticles through a stenotic electrokinetic aorta: a study on the cancer treatment", *Heat Transfer Research*, **52**, pp. 87–99 (2021).
- Prasanna Kumara, B.C. "Assessment of the local thermal non-equilibrium condition for nanofluid flow through porous media: A comparative analysis", *Indian Journal of Physics*, **96**, pp. 2475–2483 (2022).
- Prasannakumara, B.C. "Numerical simulation of heat transport in Maxwell nanofluid flow over a stretching sheet considering magnetic dipole effect", *Partial Differential Equations in Applied Mathematics*, **4**, 100064 (2021).
- Magesh, A. and Kothandapani, M. "Heat and mass transfer analysis on non-Newtonian fluid motion driven by peristaltic pumping in an asymmetric curved channel", *The European Physical Journal Special Topics*, **230**(5), pp. 1447–1464 (2021).
- Magesh, A. and Kothandapani, M. "Analysis of heat and mass transfer on the peristaltic movement of Carreau nanofluids", *Journal of Mechanics in Medicine and Biology*, **22**(01), 2150068 (2022).
- Tamizharasi, P., Vijayaragavan, R., and Magesh, A. "Heat and mass transfer analysis of the peristaltic driven flow of nanofluid in an asymmetric channel", *Partial Differential Equations in Applied Mathematics*, **4**, 100087 (2021).
- Magesh, A., Kothandapani, M., and Pushparaj, V. "Electro-osmotic flow of Jeffrey fluid in an asymmetric micro-channel under the effect of magnetic field", *Journal of Physics: Conference Series*, **1850**, pp. 012102 (2021).
- Magesh, A., Kumar, P.P., Tamizharasi, P., et al. "Effect of magnetic field on the peristaltic transport of Oldroyd-B fluid in an asymmetric inclined channel", *Journal of Physics: Conference Series*, **1850**, p. 012111 (2021).
- Ramesh, K. and Devakar, M. "Peristaltic transport of MHD Williamson fluid in an inclined asymmetric channel through porous medium with heat transfer", *Journal of Central South University*, **22**(8), pp. 3189–3201 (2015).
- Katta, R. and Jayavel, P. "Heat transfer enhancement in radiative peristaltic propulsion of nanofluid in the presence of induced magnetic field", *Numerical Heat Transfer, Part A: Applications*, **79**(2), pp. 83–110 (2020).
- Ramesh, K., Gnaneswara Reddy, M., and Devakar, M. "Biomechanical study of magnetohydrodynamic Prandtl nanofluid in a physiological vessel with thermal radiation and chemical reaction", *Proceedings of the Institution of Mechanical Engineers, Part N: Journal of Nanomaterials, Nanoengineering and Nanosystems*, **232**(4), pp. 95–108 (2018).
- Ramesh, K. and Devakar, M. "Influence of heat transfer on the peristaltic transport of Walters B fluid in an inclined annulus", *Journal of the Brazilian Society of Mechanical Sciences and Engineering*, **39**(7), pp. 2571–2584 (2017).
- Shah, S., Hussain, S., Sagheer, M., et al. "Numerical study of three-dimensional mixed convective maxwell nanofluid flow over a stretching surface with non-linear thermal radiation and convective boundary conditions", *Journal of Nanofluids*, **8**(1), pp. 160–170 (2019).
- Crooke, P.S. "On growth properties of solutions of the Saffman dusty gas model", *Zeitschrift für Angewandte Mathematik und Physik ZAMP*, **23**(2), pp. 182–200 (1972).
- Charya, G.R. "Pulsatile flow of a dusty fluid through a constricted channel", *Zeitschrift für Angewandte Mathematik und Physik ZAMP*, **29**(2), pp. 217–225 (1978).

19. Srinivasa Charya, D. and Radha Krishnama Charya, G. "The effects of wall properties on peristaltic transport of a dusty fluid", *Turkish Journal of Engineering and Environmental Sciences*, **32**(6), pp. 357–365 (2008).
20. Muthuraj, R., Nirmala, K., and Srinivas, S. "Influences of chemical reaction and wall properties on MHD peristaltic transport of a dusty fluid with heat and mass transfer", *Alexandria Engineering Journal*, **55**(1), pp. 597–611 (2016).
21. Bhatti, M.M., Zeeshan, A., Ijaz, N., et al. "Mathematical modelling of nonlinear thermal radiation effects on EMHD peristaltic pumping of viscoelastic dusty fluid through a porous medium duct", *Engineering Science and Technology, an International Journal*, **20**(3), pp. 1129–1139 (2017).
22. Tariq, H., Khan, A.A., and Zaman, A. "Peristaltically wavy motion on dusty Walters B fluid with inclined magnetic field and heat transfer", *Arabian Journal for Science and Engineering*, **44**(9), pp. 7799–7808 (2019).
23. Khan, A.A. and Tariq, H. "Influence of wall properties on the peristaltic flow of a dusty Walter's B fluid", *Journal of the Brazilian Society of Mechanical Sciences and Engineering*, **40**(8), pp. 1–18 (2018).
24. Javed, M. and Hayat, T. "Effects of heat transfer on MHD peristaltic transport of dusty fluid in a flexible channel", *International Bhurban Conference on Applied Sciences and Technology (IBCAST)*, pp. 539–550 (2017).
25. Ganesh Kumar, K., Gireesha, B.J., and Gorla, R.S.R. "Flow and heat transfer of dusty hyperbolic tangent fluid over a stretching sheet in the presence of thermal radiation and magnetic field", *International Journal of Mechanical and Materials Engineering*, **13**(1), pp. 1–11 (2018).
26. Gireesha, B.J., Mahanthesh, B., Thammanna, G.T., et al. "Hall effects on dusty nanofluid two-phase transient flow past a stretching sheet using KVL model", *Journal of Molecular Liquids*, **256**, pp. 139–147 (2018).
27. Kiran, G.R., Murthy, V.R., and Radha Krishnama Charya, G. "Pulsatile flow of a dusty fluid thorough a constricted channel in the presence of magnetic field", *Materials Today: Proceedings*, **19**, pp. 2645–2649 (2019).
28. Punith Gowda, R.J., Naveen K.R., and Prasanna Kumara, B.C. "Two-phase Darcy-Forchheimer flow of dusty hybrid nanofluid with viscous dissipation over a cylinder", *International Journal of Applied and Computational Mathematics*, **7**(3), pp. 1–18 (2021).
29. Shankaralingappa, B.M., Gireesha, B.J., Prasanna Kumara, B.C. "Darcy-Forchheimer flow of dusty tangent hyperbolic fluid over a stretching sheet with Cattaneo-Christov heat flux", *Waves in Random and Complex Media*, pp. 1–20 (2021).
30. Radhika, M., Punith Gowda, R.J., Naveenkumar, R., et al. "Heat transfer in dusty fluid with suspended hybrid nanoparticles over a melting surface", *Heat Transfer*, **50**(3), pp. 2150–2167 (2021).
31. Ali, N., Sajid, M., and Hayat, T. "Long wavelength flow analysis in a curved channel", *Zeitschrift für Naturforschung A*, **65**(3), pp. 191–196 (2010).
32. Hayat, T., Farooq, S., and Alsaedi, A. "MHD peristaltic flow in a curved channel with convective condition", *Journal of Mechanics*, **33**(4), pp. 483–499 (2017).
33. Shehzad, S.A., Abbasi, F.M., Hayat, T., et al. "Peristalsis in a curved channel with slip condition and radial magnetic field", *International Journal of Heat and Mass Transfer*, **91**, pp. 562–569 (2015).
34. Bibi, F., Hayat, T., Farooq, S., et al. "Entropy generation analysis in peristaltic motion of Sisko material with variable viscosity and thermal conductivity", *Journal of Thermal Analysis and Calorimetry*, **143**(1), pp. 363–375 (2021).
35. Nadeem, S. and Shahzadi, I. "Mathematical analysis for peristaltic flow of two phase nanofluid in a curved channel", *Communications in Theoretical Physics*, **64**(5), p. 547 (2015).
36. Riaz, A., Khan, S.U.D., Zeeshan, A., et al. "Thermal analysis of peristaltic flow of nanosized particles within a curved channel with second-order partial slip and porous medium", *Journal of Thermal Analysis and Calorimetry*, **143**(3), pp. 1997–2009 (2021).
37. Rashid, M., Ansar, K., and Nadeem, S. "Effects of induced magnetic field for peristaltic flow of Williamson fluid in a curved channel", *Physica A: Statistical Mechanics and its Applications*, **553**, 123979 (2020).

Biographies

Hadia Tariq obtained her PhD degree from International Islamic University, Islamabad in 2020. She is currently serving as Assistant Professor in National University of Modern Languages, Islamabad in Department of Mathematics. Her area of interest is fluid mechanics.

Ambreen Afsar Khan received her PhD degree from Quaid-i-Azam University, Islamabad in 2007. She is working as Assistant Professor in International Islamic University, Islamabad in Department of Mathematics and Statistics. Her area of specialization is fluid mechanics.

Sajid Shah received his PhD degree from Capital University of Science and Technology, Islamabad in 2019. He is working as Assistant Professor in Government Postgraduate College, Asghar Mall, Rawalpindi in the Department of Mathematics. His area of specialization is fluid mechanics.